UWA360CAM: A 360° 24/7 Real-Time Streaming Camera System for Underwater Applications

Quan-Dung Pham[1], Yipeng Zhu[1], Tan-Sang Ha[1], K.H. Long Nguyen[1], Binh-Son Hua[2], and Sai-Kit Yeung[1]

Abstract—**Omnidirectional camera is a cost-effective and information-rich sensor highly suitable for many marine applications and the ocean scientific community, encompassing several domains such as augmented reality, mapping, motion estimation, visual surveillance, and simultaneous localization and mapping. However, designing and constructing such a high-quality 360° real-time streaming camera system for underwater applications is a challenging problem due to the technical complexity in several aspects including sensor resolution, wide field of view, power supply, optical design, system calibration, and overheating management. This paper presents a novel and comprehensive system that addresses the complexities associated with the design, construction, and implementation of a fully functional 360° real-time streaming camera system specifically tailored for underwater environments. Our proposed system, UWA360CAM, can stream video in real time, operate in 24/7, and capture 360° underwater panorama images. Notably, our work is the pioneering effort in providing a detailed and replicable account of this system. The experiments provide a comprehensive analysis of our proposed system.**

I. INTRODUCTION

Comprehending the utilisation of habitats by species and the diversity of such habitats are of significant importance in the fields of ecology and conservation, both in marine and terrestrial ecosystems. Moreover, the ocean encompasses a substantial volume and represents the most extensive viable ecosystem on the planet. However, the acquisition of data pertaining to these aspects is frequently challenging. Color camera is an affordable and data-intensive sensor that is well suited for several marine applications, including the detection of aquatic animals, estimation of motion, coral cultivation and monitoring [1], [2].

Acquiring global scene information is important to understand our 3D environment [3], which can be implemented using an omnidirectional visual representation that encompasses a full 360° view along the vertical axis at every point of observation [4]. A traditional approach to obtain omnidirectional sensing relies on heavy and unreliable mechanical structures [5], e.g., the construction of an omnidirectional stereo system using plane mirrors [6]. Another potential approach is to install additional cameras [5], but this approach has financial implications and suffers from limitations in the architectural framework. A modern cost-effective approach is to instead use catadioptric cameras or fisheye cameras, which offer wider field of view for enhanced environmental coverage [7], [8], and thus the ability to capture panoramic views [9], [10]. Additionally, some recent studies [11], [12], [13] demonstrated promising results of omnidirectional depth estimation using fisheye images. Omnidirectional panoramic video systems therefore find extensive employment in various domains, including virtual reality, 360° movies, and video surveillance [14].

For submerged environments, the utilisation of omnidirectional cameras has numerous novel technological possibilities across a range of disciplines, including underwater robotics, marine science, oil and gas sectors, underwater archaeology, and public outreach. Nevertheless, the utilisation of these cameras remains significantly restricted compared to their use in the air and on land, mostly due to the inherent difficulties posed by the underwater environment. Numerous camera models have been suggested to offer projection and unprojection functionalities that are well-suited for accommodating large field-of-view lenses [15]. However, previous studies have failed to address all-encompassing optical concerns inside the underwater setting.

In this paper, a new system is proposed with a detailed pipeline for design, construction, and implementation of a fully functional 360° camera suitable for real-time streaming in underwater environments. The main contributions of this work are:

- A comprehensive hardware and software pipeline for the development of a complete underwater camera system capable of capturing a full 360° field of view and continuously stream in 24/7. This promotes further investigation into the construction of high-quality underwater camera systems with a 360° field of view.
- A system that takes into account perspective projection and refraction of water, pressure housings and air for underwater applications. By employing this method, it is possible to more accurately estimate the imaging process and obtain optimal levels of precision.
- Extensive experiments to analyze the performance of our proposed 360° camera system.

To our knowledge, this is the most comprehensive documentation to date in the research community to detail the design of a 360° camera system for underwater applications.

II. UWA360CAM SYSTEM OVERVIEW

The UWA360CAM system comprises three distinct components as in Fig. 1, namely an underwater camera module, a transmission module, and a topside computer processing module. The design of the proposed system is shown in Fig. 2a. The camera operates in three main stages: 1) The initial stage of the system triggers the fisheye cameras in a synchronised manner. 2) In the subsequent stage, the onboard processing unit allows the transmission of the images to the

---

[1]Hong Kong University of Science and Technology, Hong Kong SAR.
[2]Trinity College Dublin, Ireland.
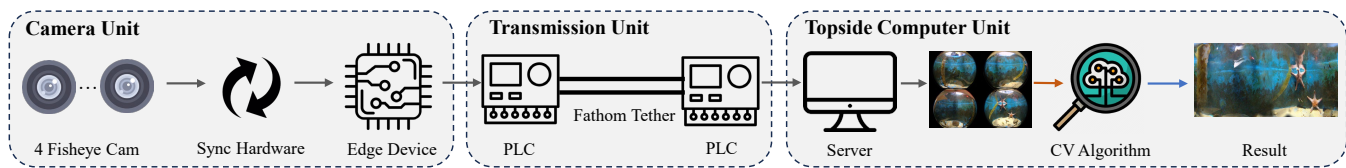
Fig. 1: Our system functions in three main stages: 1) The camera unit triggers the fisheye cameras in a synchronised manner. 2) The transmission unit sends the images to the server via Fathom Tether. 3) The high-performance server performs computer vision algorithms such as image stitching.

server. 3) The last stage is executed on a high-performance server to accommodate advanced computer vision algorithms such as video stitching.

Our proposed system employs four fisheye cameras, which provides a bare minimum data acquisition that allows us to obtain 360° depth image. The design of the system involves the placement of a set of fisheye cameras in a configuration where two cameras are positioned in a front-backward orientation at the top, and another set of fisheye cameras is positioned at the bottom in a perpendicular direction as shown in Fig. 2b. This arrangement ensures that each adjacent pair of stereo cameras maintains an equal baseline distance. In order to synchronise multiple fisheye camera, a hardware board is used to allow for the connection of four same MIPI cameras and a software is developed to send a frame whenever the host places a request. The camera remains in a condition of continuous operation, and upon receiving a request from the host, it transmits the frame to facilitate synchronisation. The delay is contingent upon the performance of the host device. Hence, in instances where host devices exhibit sub-optimal performance, it is quite probable that latency will exhibit fluctuations. At the heart of our system, a Jetson Nano board is used to communicate with the synchronised fisheye cameras for processing and transmiting images. Power Line Communication (PLC) modules are employed through the use of Fathom Tether in order to supply power and transmit video data from an underwater camera to a computer located above the water's surface. Finally, the high-performance computer is used for the implementation of advanced computer vision algorithms that process input videos obtained from four synchronised fisheye cameras.

III. HARDWARE

A. Cameras and Fisheye Lens

When choosing the appropriate camera sensor for underwater applications, it is essential to consider many aspects including a high level of resolution to effectively capture photos of marine organisms, a high signal-to-noise ratio in order to guarantee the production of clear images, an adequate dynamic range to capture both the brighter and darker regions within the scene. In our research, four SONY IMX477 sensor cameras are utilised since it offers high-resolution, high-speed image sharpness, improved low-light performance, and high sensitivity. The IMX477 provides the maximum resolution of 4056×3040, the maximum framerate

60fps, pixel size $1.55 \mu m \times 1.55 \mu m$, optical format 1/2.3", and the high-performance MIPI CSI-2 interface offers a maximum bandwidth of 10 Gb/s with four image data lanes and uses fewer CPU resources. The IMX477 image sensor offers a mechanical IR cut-off filter switched automatically based on light condition which is only visible light during the bright light and infrared sensitivity during low light condition. The cameras are oriented in four distinct directions in order to establish both horizontal and vertical baselines as shown in Fig. 2b. To maximize the field of view, 220° fisheye lens is utilized, which is among the widest options available in the market.

B. Processing Unit and Synchonized Cameras Unit

The processing unit is responsible for the three primary functions. The first objective is to transmit the control signal to four fisheye cameras in order to facilitate the simultaneous capture of images or video recording. The second objective involves doing pre-processing on the images prior to their transmission to the topside computer via the transmission unit. The final step involves transferring images or streaming videos to the server in order to facilitate the application of more sophisticated computer vision algorithms such as video stitching and fish detection. It is essential to take into account the significance of a high processing speed and considerable bandwidth in order to effectively transmit high-resolution content with a frame rate of at least 24 frames per second to meet the need for real-time streaming. In this paper, a low-cost edge device is utilized, the NVIDIA Jetson Nano, which provides 4 GB 64-bit LPDDR4, 1600MHz 25.6 GB/s, and MIPI CSI-2 D-PHY 1.1 interfaces. For Multi-Stream HD Video, Jetson Nano can support up to H.264 2160p 60fps. A particular challenge of a multi-camera system is its synchronization mechanism in order to ensure all frames are captured at the same timestamp. To synchronize our fisheye cameras, a synchronized 4-camera hardware is used. The purpose of this hardware board is to provide the simultaneous connection of four identical MIPI cameras. Additionally, a firmware has been built to enable the transmission of a frame whenever the host initiates a request. The camera maintains a state of uninterrupted functioning, and when prompted by the host, it transmits the frame to enable synchronisation.

C. Communication

To stream video from underwater camera unit to topside computer unit with high-resolution video at 24 fps, it is necessary to take into account waterproof wire communication.
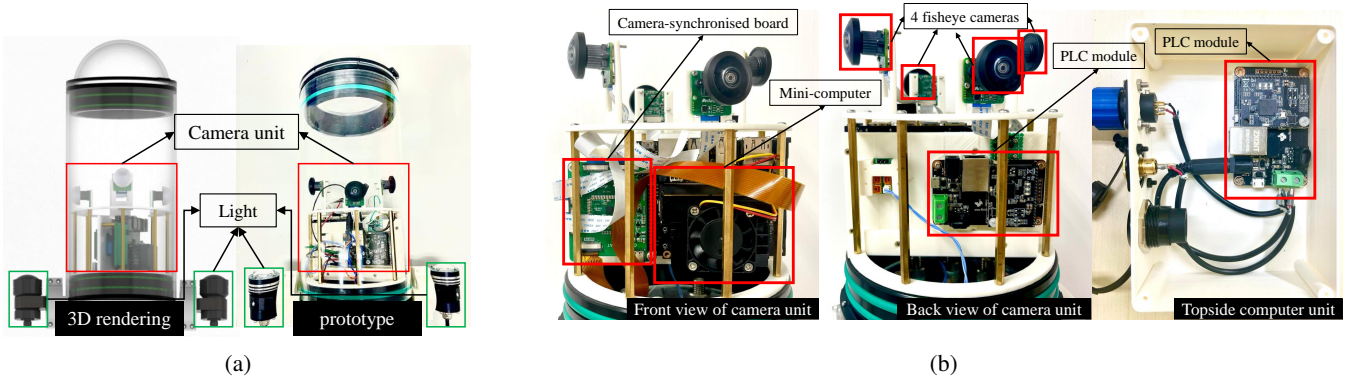
Fig. 2: Overview of our 360° underwater camera. (a) 3D rendering and real-world prototype of our system. (b) Front view (left) and back view (middle) of our system with fisheye cameras, a camera-synchronized board and a computing unit. Topside computer unit (right) contains the PLC module.

To avoid additional cables and costs, it is proposed to use Power Line Communication. The Fathom Tether is used as Fig. 3a, a high-quality tether cable designed specifically for subsea applications [16], to transmit data from an offshore NVIDIA Jetson Nano to an onshore server. It is neutrally buoyant, has 300–350lb breaking strength, and is embedded with water-blocking fibers to seal any leaks. In order for the Fathom Tether to work well for tether lengths of up to 100m, it is necessary to utilize the Power Line Communication modules as illustrated in Fig. 2b. It is based on the Qualcomm QCA7420 SoC, which takes advantage of the robust HomePlug AV (IEEE-1901) standard to send Ethernet through powerlines. It offers MA data rate up to 500 Mbps and 128-bit AES data encryption. The Real-Time Streaming Protocol (RTSP) is employed to facilitate the transmission of real-time video with minimal latency. This protocol enables the streaming of video content from an edge device located offshore to a server situated onshore.

D. Enclosure

Our custom mechanical enclosure design effectively protects the onboard processing module and cameras from water leakage and avoids undesirable optic effects during functioning. The propagation of light involves traversing three distinct environments with different reflective indexes, namely water, a cast acrylic cage, and air, prior to reaching the camera sensor. This sequential passage through several environments introduces a refraction effect. The influence of refraction on the calibration of the camera system is a significant consideration, and therefore, it is addressed in the subsequent section for calibration purposes. Furthermore, the selection of acrylic material is made in order to ensure the system's ability to withstand high pressure conditions of up to 100 metres in depth.

In order to mitigate the problem of overheating during operation, the enclosure has a thermal forced convection mechanism that utilises 50% of its internal volume. Given the elevated temperatures experienced during the operation of cameras and CPUs, it is common practice to employ a fan
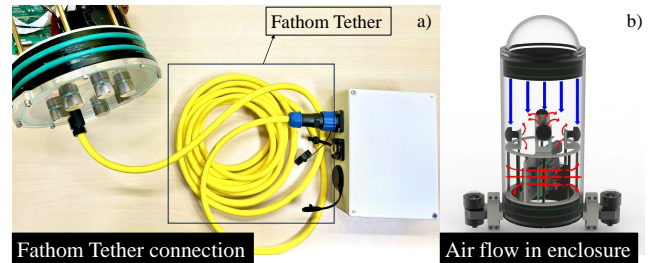
Fig. 3: a) Fathom Tether connection between camera unit and topside computer unit and b) Air flow in enclosure designed for forced convection.

to induce air circulation within the system, which enables efficient transportation of substantial amounts of thermal energy. The elevated temperature air emanating from the camera and CPU will be conveyed to the vacant space within the tube as shown in Fig. 3b. This leads to a decrease in the temperature of the system, which mitigates the problem of overheating. In our implementation, the proposed camera system is capable of uninterrupted operation for a duration of 24/7.

IV. SOFTWARE

A. Fisheye Camera Model

To produce a 360° panoramic view in our system, it is necessary to model the image formation for a fisheye camera. There exists some criteria to select a camera model for our system. First, it is desirable to have a camera model specifically designed for fisheye lenses to account for the strong visual distortion on fisheye images. Such distortions must be modeled for both the project and unproject function to map a 3D point to a 2D pixel and vice versa so that the camera model can support tasks such as depth estimation as well. Second, it is preferred to have a camera model with a simple and precise calibration and high-quality 3D reconstruction procedure. In the literature, Scaramuzza *et al.* [17] present a camera projection model that uses high-order polynomials
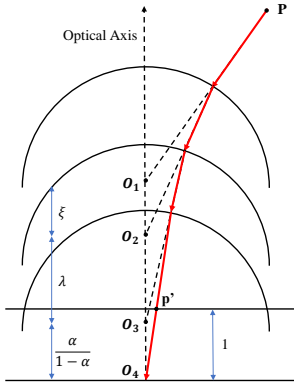
Fig. 4: Triple Sphere camera model. The incident light ray from a point P travels through water, the acrylic enclosure, and the air into the sensor

to represent distortions. This model exhibits a high level of generality and can be effectively used with a range of catadioptric and fisheye cameras. However, due to the absence of a closed-form solution, it becomes necessary to approximate the inverse projection equation using a high-order polynomial, resulting in the introduction of errors. The unified camera model (UCM) [18] is general for modeling catadioptric cameras and fisheye cameras with an enhanced calibration accuracy provided by the MUCM model [19]. Recently, the Double Sphere camera model [15] is a new model that has only one more intrinsic parameter than the MUCM model but with substantial calibration accuracy improvement. However, these models did not consider underwater applications that involve light refraction effects. In this work, it is proposed to use the Triple Sphere camera model (TSCM) [20] because TSCM can accurately model the image formation of fisheye cameras stored in an enclosure and placed underwater. It is assumed that the enclosure possesses a slender thickness, and therefore the light transport can be modeled by an incident light ray traversing in the water and undergoing a single refraction off the housing before reaching the camera. This camera model calibration is highly effective in handling wide field of view (FOV) angles that exceed 180°. This method has achieved precisely to calibrate intrinsic parameters in underwater application since it takes into account the refraction when incident light travel through water, enclosure and air.

Fig. 4 shows our camera model. TSCM is a projection model based on the so-called DSCM model. Particularly, the camera projection model considers the incident light refracting three times including once through water to camera and the other two times due to the double sphere camera. Let scalar α, ξ and λ be the displacements of the three unit spherical centers. Let $\Omega \subset \mathbb{R}^3$ and $\Theta \subset \mathbb{R}^2$ denotes the set of 3D points that result in valid projections and the image domain to which points can be projected to, respectively. The camera projection function is defined by $\pi_c : \Omega \mapsto \Theta$, which models the relationship between points in the 3D space and pixels on the image plane. The unprojection model

$\pi_c^{-1} : \Theta \mapsto \mathbb{R}^3$ inverts a pixel to an outgoing ray into the 3D space.

Given a 3D point $\mathbf{P} = [X,Y,X]^T \in \mathbb{R}^3$, the projection function of the camera can be defined as

$$\pi_{\mathbf{c}}(\mathbf{P},\mathbf{i}) = \frac{1}{\phi} \begin{bmatrix} f_x & 0 & c_x \\ 0 & f_y & c_y \end{bmatrix} \begin{bmatrix} X \\ Y \\ \phi \end{bmatrix} \tag{1}$$

$$\phi = Z + \xi d_0 + \lambda d_1 + \frac{\alpha}{1-\alpha} d_2 \tag{2}$$

$$d_0 = \sqrt{X^2 + Y^2 + Z^2} \tag{3}$$

$$d_1 = \sqrt{X^2 + Y^2 + (\xi d_0 + Z)^2} \tag{4}$$

$$d_2 = \sqrt{X^2 + Y^2 + (\xi d_0 + \lambda d_1 + Z)^2} \tag{5}$$

where $\mathbf{i}$ is the vector of intrinsic parameters. A set of 3D points that results in valid projection is expressed as follows:

$$\Omega = \{x \in \mathbb{R} \mid z > -w_2 d_0\} \tag{6}$$

$$w_2 = \frac{\xi + \lambda + w_1}{\sqrt{1 + (\xi+\lambda)^2 + 2w_1(\xi+\lambda)}} \tag{7}$$

$$w_1 = \frac{\alpha}{1-\alpha} \tag{8}$$

The unprojection function is computed as follows:

$$\pi_{\mathbf{c}}^{-1}(\mathbf{p},\mathbf{i}) = \mu \begin{bmatrix} \eta \gamma x \\ \eta \gamma y \\ m_z \end{bmatrix} - \begin{bmatrix} 0 \\ 0 \\ \xi \end{bmatrix} \tag{9}$$

$$\mu = \xi m_z + \sqrt{\xi^2 m_z^2 - \xi^2 + 1} \tag{10}$$

$$m_z = \eta(\gamma - \phi) - \lambda \tag{11}$$

$$\eta = \lambda(\gamma - \phi) + \sqrt{\lambda^2(\gamma-\phi)^2 - \lambda^2 + 1} \tag{12}$$

$$\gamma = \frac{\phi + \sqrt{1 + (1-\phi^2)(x^2+y^2)}}{x^2 + y^2 + 1} \tag{13}$$

$$\phi = \begin{cases} \dfrac{\alpha}{1-\alpha} & \text{if } \alpha \le 0.5 \\ \dfrac{1-\alpha}{\alpha} & \text{if } \alpha > 0.5 \end{cases} \tag{14}$$

where (x,y) is the normalized coordinate.

B. Camera Calibration

To calibrate this camera model, corners are detected in the calibration board and minimise the reprojection error of the corner points across all images. The projection point u_{nk} of the kth corner x_k can be obtained using the corner detector for each picture n in the calibration sequence. The coordinate of u_{nk} is related to the camera intrinsic and extrinsic parameters. Let us denote $s = [\mathbf{i}, \mathbf{T}_{\mathbf{cam_0}}, \mathbf{T}_{\mathbf{cam_1}}, \dots \mathbf{T}_{\mathbf{cam_n}}]$ the parameter to optimize. It can be constructed the nonlinear optimization problem as follows:

$$s^* = \arg\min_s \sum_{n=0}^{N} \sum_{k \in K} \rho\left((\pi(\mathbf{T}_{\mathbf{cam_n}} \mathbf{x_k}, \mathbf{i} - u_{nk}))^2\right) \tag{15}$$

where $\mathbf{T}_{\mathbf{cam_n}} \in SE(3)$ is the transformation from the coordinate frame of the calibration grid to the camera coordinate frame for image n. K is a set of detected corner points

for the image n and ρ is the robust Huber norm. Since the optimization is non-convex, good initialization of the intrinsic parameter $\mathbf{i}$ and camera poses $\mathbf{T_{cam}}$ is important for optimization to converge. The intrinsic parameters is initialized with using the method [21] and find initial poses using the UPnP algorithm [22].

C. Real-time Panorama Stitching

To make the system suitable for streaming, it is expected panorama stitching to run in real time. The panorama stitching method is adopted from Fast Sphere Sweeping Stereo [13], which has many useful properties suitable for underwater tasks and can be modified for coping with multiple fisheye cameras and light refraction. Our stitching algorithm has three stages. 1) First, adaptive spherical matching is used to perform stereo matching on the fisheye images, while taking into account the regional discriminative capability of distance inside each fisheye image. 2) Second, an efficient spherical cost aggregation method with optimal complexity $O(n)$ is performed to allow a stable sphere sweeping volume in noisy and textureless regions. This method can preserve edges with a coverage of $360°$. 3) Finally, distance-aware stitching is employed to generate a $360°$ panorama by integrating colours from several distance maps. This is achieved through efficient inpainting techniques.

In our stitching algorithm, spherical matching is a critical but also computationally expensive step as it requires to evaluate the whole depth candidates in all the combinations of overlapping regions along the baseline within the sphere sweeping volume. To achieve real-time performance, given a reference camera, a camera selection approach is employed to identify the most suitable camera pairs for correspondence search within the sphere sweeping volume. The optimal camera c^* for each pixel in the reference is determined by

$$c^*(\theta, \phi) = \arg\max_{c_k}(q_{c_k}) \qquad (16)$$

where q_{c_k} is the angular change between two 3D points $p_{c_k}^{<0>}$ and $p_{c_k}^{<N-1>}$; 0 and $N-1$ are the first and last layer of the sphere sweeping volume.

Our adaptation of spherical matching to the Triple Sphere camera model is as follows. In typical conditions outside, the spherical matching can be easily achieved by utilising the camera's intrinsic parameter matrix from Double Sphere Camera Model. Nevertheless, the process of capturing images underwater becomes significantly more complex due to the need to consider the impact of the refractive interface. To measure the distance for distance discriminating in order to solve Eq. 16 for the Triple Sphere camera model, it is performed two $220°$ distance estimation using the two opposed top cameras as two references. For each pixel in each reference, the best camera is selected using selective matching. Let I_{c_s} be the image from the camera selected at pixel (θ, ϕ) and I_{c_0} be the reference camera. The matching cost for the i_{th} distance candidate is:

$$C(\theta, \phi, i) = \|V_{c_s \mapsto c_0}(\theta, \phi, i) - I((\theta, \phi)\|_1 \qquad (17)$$

where $V_{c_s \mapsto c_0}$ is the sphere sweeping volume from the selected camera to the reference camera.

Then each slice of the spherical cost volume is regularized using a fast filtering method. To aggregate sparse distance to obtain a dense distance map, first downsample is used with an edge preservation filter using the bilateral weights between the guidance center and the neighbor pixels. The bilateral weights are:

$$w_{mn}(I, x, y) = \exp\left(\frac{\|I(x, y) - I(x+m, y+m)\|^2}{2\sigma_I^2} \right) \qquad (18)$$

where σ_I is the edge preservation parameter, and (x, y) are pixel coordinates. The downsampling operation can then be defined by

$$I(x, y) = \sum_{m,n=-1}^{1} I(2x+m, 2y+m) w_{m,n}(I, 2x, 2y)/\tau \qquad (19)$$

where τ is the normalizing constant. Then upsampling is performed using a minimal pixel support. Guidance weights are computed between the guidance centers and the pixels to aggregate at lower scale. After cost volume filtering, the optimal distance is voted via winner-takes-all, and sub-candidate accuracy is achieved through quadratic fitting.

Although this methodology results in improved precision, an additional procedure is necessary to combine the fisheye images. This method involves initially generating a distance map at a specified position, followed by projecting the image based on the corresponding 3D coordinates. Subsequently, the images are merged using a blending technique that assigns greater importance to pixels with little displacement.

V. EXPERIMENTAL EVALUATION

Our proposed system is configured with a Fathom Tether cable of 10-meter length and let the system operate continuously in 48 hours. It is aimed at evaluating the system temperature and operational performance while it is functioning. Also, evaluation of the calibration of our system is conducted.

Table I reports the capability of our camera system in details. The proposed system offers high video framerate at 30 fps, high-resolution image capture at 2028×1520 and a low latency of 5 ms, which is suitable for real-time application and environment monitor. This camera system also offers 12 bits color depth and HDR.

Specification	
Frame rates	30 fps
Resolution	2028×1520
Stream time	24 hours
Latency	5 ms
Synchronization	YES
FOV	360(H), 180(V)
Optical Format	1/2.3"
Color depth	12 bits
HDR	YES

TABLE I: Camera specifications
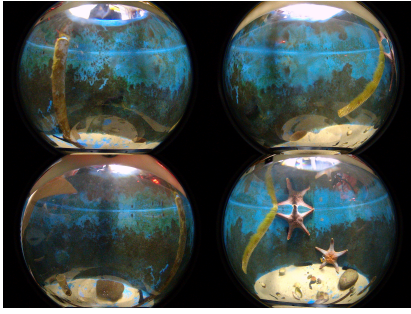
(a) Captured images using our proposed method

(b) Stitched panorama image using adapted FSSS algorithm

Fig. 5: The images taken by camera system and 360° panorama image stitching using images taken by camera system
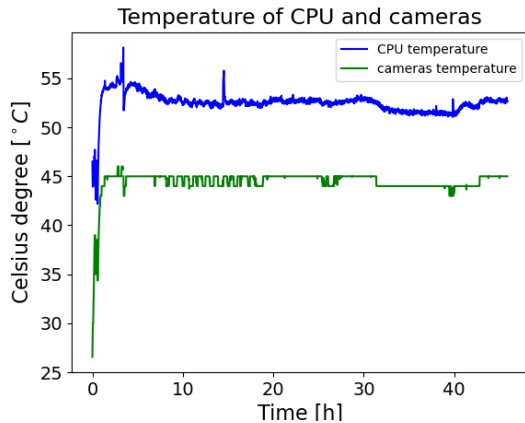
Fig. 6: Temperatures of CPU and cameras in 48 hours

Camera	DSCM Error ↓	TSCM Error ↓
1	2.12	2.11
2	1.89	1.81
3	3.45	3.26
4	1.65	1.58
Average	2.28	2.19

TABLE II: Mean reprojection error for evaluated camera models between DSCM and TSCM (in pixels)

A. Operational Performance

Fig. 5a shows the pictures taken by the proposed system in a water tank for monitoring aquatic creatures such as star fishes. Qualitatively, it is illustrated that the pictures taken by this system are clear and high-quality in underwater environment. In addition to the image quality, further analysis the system temperature is conducted, which is a crucial aspect for performance because high temperature can affect the overall stability of the system. In the event that the system experiences excessive heat, it might result in malfunctions, decreased frames per second (FPS), or even abrupt shutdown. Fig. 6 shows the temperatures of the edge device and cameras during functioning. It is evident that within the initial two-hour period, there is a significant rise in temperature for both the CPU and cameras, with the former increasing from $42.5°C$ to $54°C$, and the latter increasing from $26.5°C$ to $45°C$. Due to the forced convection in our airflow design, it is found that the CPU and camera temperatures have a tendency to remain stable subsequently.

B. Camera Calibration Accuracy

The performance of our camera calibration is reported in Table II. It can be seen that the mean reprojection error of the TSCM camera model is smaller than DSCM's. In our calibration, the coordinates of the corners of the calibration pattern are calculated by optimising for both posture and intrinsic characteristics. The TSCM with totally 7 camera internal parameters demonstrates better reprojection error than that of the DSCM with six parameters.

C. Image Stitching Results

Fig. 5b demonstrates the qualitative result of our 360° image stitching algorithm. The running time of each frame is approximately 33*ms* on an NVIDIA RTX3090 GPU. This result is measured with real data collected at the Ocean Research Facility of the Hong Kong University of Science and Technology using the proposed camera system.

VI. CONCLUSIONS AND FUTURE WORK

This paper presents a complete hardware and software framework for the creation of an all-encompassing underwater camera system with the ability to capture a complete 360° field of view. Our system can function in real time underwater continuously. Our work encourages additional exploration of underwater camera systems with a wide field of view.

The proposed system has some limitations to be addressed in future work. First, since there are no data for underwater omnidirectional depth estimation, it is worth building a new dataset for this research and developing more accurate and reliable image stitching and depth estimation for this proposed system. Second, the enclosure design can be improved to avoid light reflection and refraction effects. Finally, it is interesting to explore a mechanical design to keep the system balanced in the water. It is planed to integrate this system with BlueROV2 to develop navigation techniques, e.g., SLAM, for underwater robots.

REFERENCES

[1] V.-N. Tran, Q.-D. Pham, T.-S. Ha, Y. H. Wong, and S.-K. Yeung, "A novel platform to control biofouling in pearl oysters cultivation," in *2023 IEEE International Conference on Robotics and Automation (ICRA)*. IEEE, 2023, pp. 7447–7453.

[2] Q.-T. Truong, T.-A. Vu, T.-S. Ha, J. Lokoč, Y. H. W. Tim, A. Joneja, and S.-K. Yeung, "Marine video kit: A new marine video dataset for content-based analysis and retrieval," in *MultiMedia Modeling - 29th International Conference, MMM 2023, Bergen, Norway, January 9-12, 2023*. Springer, 2023.

[3] H. Ishiguro, M. Yamamoto, and S. Tsuji, "Omni-directional stereo," *IEEE Transactions on Pattern Analysis & Machine Intelligence*, vol. 14, no. 02, pp. 257–262, 1992.

[4] H.-C. Huang and Y.-P. Hung, "Spisy: The stereo panoramic imaging system," in *Third Workshop on Real-Time and Media Systems*. Citeseer, 1997, pp. 71–78.

[5] J. Shimamura, N. Yokoya, H. Takemura, and K. Yamazawa, "Construction of an immersive mixed environment using an omnidirectional stereo image sensor," in *Proceedings IEEE Workshop on Omnidirectional Vision (Cat. No. PR00704)*. IEEE, 2000, pp. 62–69.

[6] F. Zhou, X. Chai, X. Chen, and Y. Song, "Omnidirectional stereo vision sensor based on single camera and catoptric system," *Applied optics*, vol. 55, no. 25, pp. 6813–6820, 2016.

[7] J. Courbon, Y. Mezouar, L. Eckt, and P. Martinet, "A generic fisheye camera model for robotic applications," in *2007 IEEE/RSJ International Conference on Intelligent Robots and Systems*. IEEE, 2007, pp. 1683–1688.

[8] Y.-C. Huang, C.-W. Liu, and J.-H. Chuang, "Using fisheye camera for cost-effective multi-view people localization," in *2021 IEEE International Conference on Image Processing (ICIP)*. IEEE, 2021, pp. 3248–3252.

[9] W. Li and Y. F. Li, "Single-camera panoramic stereo imaging system with a fisheye lens and a convex mirror," *Optics express*, vol. 19, no. 7, pp. 5855–5867, 2011.

[10] J. Gluckman, S. K. Nayar, and K. J. Thoresz, "Real-time omnidirectional and panoramic stereo," in *Proc. of Image Understanding Workshop*, vol. 1. Citeseer, 1998, pp. 299–303.

[11] C. Won, J. Ryu, and J. Lim, "Omnimvs: End-to-end learning for omnidirectional stereo matching," in *Proceedings of the IEEE/CVF International Conference on Computer Vision*, 2019, pp. 8987–8996.

[12] ——, "Sweepnet: Wide-baseline omnidirectional depth estimation," in *2019 International Conference on Robotics and Automation (ICRA)*. IEEE, 2019, pp. 6073–6079.

[13] A. Meuleman, H. Jang, D. S. Jeon, and M. H. Kim, "Real-time sphere sweeping stereo from multiview fisheye images," in *CVPR*, June 2021.

[14] R. Al-Harasis and B. H. Sababha, "On the design and implementation of a dual fisheye camera-based surveillance vision system," *Multimedia Tools and Applications*, vol. 78, pp. 22 667–22 689, 2019.

[15] V. Usenko, N. Demmel, and D. Cremers, "The double sphere camera model," in *2018 International Conference on 3D Vision (3DV)*. IEEE, 2018, pp. 552–560.

[16] "Bluerobotics fathom rov tether," https://bluerobotics.com/store/cables-connectors/cables/fathom-rov-tether-rov-ready/[Accessed: July 1, 2023].

[17] D. Scaramuzza, A. Martinelli, and R. Siegwart, "A toolbox for easily calibrating omnidirectional cameras," in *2006 IEEE/RSJ International Conference on Intelligent Robots and Systems*. IEEE, 2006, pp. 5695–5701.

[18] S. Baker and S. K. Nayar, "A theory of single-viewpoint catadioptric image formation," *International journal of computer vision*, vol. 35, pp. 175–196, 1999.

[19] C. Mei and P. Rives, "Single view point omnidirectional camera calibration from planar grids," in *Proceedings 2007 IEEE International Conference on Robotics and Automation*. IEEE, 2007, pp. 3945–3950.

[20] S. Xie, D. Wang, and Y.-H. Liu, "Omnividar: Omnidirectional depth estimation from multi-fisheye images," in *Proceedings of the IEEE/CVF Conference on Computer Vision and Pattern Recognition*, 2023, pp. 21 529–21 538.

[21] L. Heng, G. H. Lee, and M. Pollefeys, "Self-calibration and visual slam with a multi-camera system on a micro aerial vehicle," *Autonomous robots*, vol. 39, pp. 259–277, 2015.

[22] L. Kneip, H. Li, and Y. Seo, "Upnp: An optimal o (n) solution to the absolute pose problem with universal applicability," in *Computer Vision–ECCV 2014: 13th European Conference, Zurich, Switzerland, September 6-12, 2014, Proceedings, Part I 13*. Springer, 2014, pp. 127–142.